Acta Oceanol. Sin., 2018, Vol. 37, No. 9, P. 99–106
DOI: 10.1007/s13131-018-1269-2
http://www.hyxb.org.cn
E-mail: hyxbe@263.net

A novel ocean bathymetry technology based on an unmanned surface vehicle

JIN Jiucai[1]*, ZHANG Jie[1], SHAO Feng[1, 2], LYU Zhichao[1, 3], WANG Dong[1, 4]
[1] The First Institute of Oceanography, State Oceanic Administration, Qingdao 266061, China
[2] College of Information and Control Engineering, China University of Petroleum, Qingdao 266580, China
[3] College of Underwater Acoustic Engineering, Harbin Engineering University, Harbin 150001, China
[4] College of Electronics and Information Engineering, Harbin Institute of Technology, Harbin 150006, China

Received 22 December 2017; accepted 26 February 2018

Abstract
In ocean bathymetry, the instantaneous depth measured by survey ships or by unmanned surface vehicles (USVs) cannot be directly taken as the chart depth because of the effect of waves and the tide. A novel ocean bathymetry technology is proposed based on the USV, the aim is to evaluate the potential of the USV using a real-time kinematic (RTK) and a single beam echo sounder for ocean bathymetry. First, using the RTK height of the USV with centimeter-level precision, the height of the sea level is obtained by excluding wave information using a low pass filter. Second, the datum distance between the reference ellipsoid and the chart depth is obtained by a novel method using tide tables and the height of the sea level from the USV. Previous work has usually achieved this using long-term tidal observation from traditional investigations. Finally, the chart depth is calculated using the transformation between the instantaneous depth of the USV measurement and the datum of the chart depth. Experiments were performed around the Wuzhizhou Island in Hainan Province using the unmanned surface bathymetry vehicle to validate the proposed technology. The successful results indicate the potential of the bathymetry technology based on the USV.

Key words: unmanned surface vehicle, bathymetry, attitude correction, tidal observation

Citation: Jin Jiucai, Zhang Jie, Shao Feng, Lyu Zhichao, Wang Dong. 2018. A novel ocean bathymetry technology based on an unmanned surface vehicle. Acta Oceanologica Sinica, 37(9): 99–106, doi: 10.1007/s13131-018-1269-2

1 Introduction

An unmanned surface vehicle (USV) is a novel unmanned surface platform used for surveying that has been the focus of unmanned vehicle research following the well-known unmanned aerial vehicle (UAV) and the autonomous underwater vehicle (AUV). In the future of three-dimensional unmanned observation systems, the USV can play a role as a communication medium between the UAV and the AUV. In recent years, more USVs have been designed and built, which have been applied to, for example, environmental monitoring, surveys, and acoustic communication.

In the field of bathymetry, in particular, the USV has some advantages in several aspects, such as efficiency, autonomy, cost, and security. A prototype USV ARTEMIS for bathymetry, using a new generation of navigation sensors including GPS and a digital compass, was developed by MIT in the 1990s, which can be taken as the earliest application of USV in river bathymetry (Rodriguez-Ortiz, 1996). On the basis of the ARTEMIS technology, a differential GPS (DGPS) receiver was added to the succeeding USV at MIT, known as AutoCat, to enhance the navigation system. The USVs driven by electricity and fuel dynamic systems were tested separately for river bathymetry (Manley et al., 2000). BathyBoat was designed to serve as a bathymetry platform by the University of Michigan in 2008 and is suitable for surveying the bathymetry of shallow areas because of the small hull with a draft of 0.10 m (Brown et al., 2010). Charlie, integrated with multibeam and side-scan sonars, was designed by CNR-ISSIA, and was applied to ocean surveying and the search for mine-like objects in 2010 (Bruzzone et al., 2011). A lightweight Sonobot for shallow water hydrographic surveys was built by Evologics Corp., and was tested by carrying a single beam echo sounder and a side scan sonar in a lake in 2013 (Kebkal et al., 2014). A series of the USVs that were integrated with multibeam sonar, side-scan sonar, and a single beam echo sounder were produced by SeaRobotics Corp. The USVs were tested by sea trials in the Bedford Basin (Halifax, Canada) in 2011 (Seto and Crawford, 2015). An unmanned surface bathymetry vehicle (USBV) was developed at The First Institute of Oceanography of the State Oceanic Administration of China for use in lake and sea bathymetry missions in China (Lü et al., 2016; Jin et al., 2013, 2016). The vehicles are integrated with a single beam echo sounder, GPS, and a digital compass. An USV built by the Shanghai Maritime University was tested for depth and current velocity measurements in 2015 (Zhu et al., 2016).

The integration and control technologies of the USVs are mainly studied by the above research organizations and USV companies (Annamalai et al., 2015; Shojaei, 2015; Liu et al.,

Foundation item: The National Key Research and Development Program of China under contract No. 2017YFC1405203; the National Natural Science Foundation of China under contract No. 61401111; the Public Science and Technology Research Funds Projects of Ocean of China under contract No. 201505005-2.
*Corresponding author, E-mail: jinjiucai@fio.org.cn

2016). However, methods for data processing in USV applications are rarely included in such research. In the bathymetry application, in particular, the technology required for the bathymetry in a lake and ocean is different. In the lake survey, the instantaneous depth measured by an USV using an echo sounder following a draft correction can be taken as the depth of the lake (Brown et al., 2010; Bibuli et al., 2014). However, an instantaneous depth of an USV is meaningless and useless in an oceanic survey because it contains wave and tidal information. Previous bathymetry measurements carried out on survey ships have combined the real-time kinematic (RTK) and echo sounders as the latest generation of the bathymetry technology. Because of the height measurement with high precision at centimeter - level for the RTK, the depth measurement can be accomplished without tidal observations (Hostache et al., 2015). However, applying the bathymetry technology without tidal observations directly in the USV causes some difficulties and disadvantages in the calculation of, for example, the height of the sea level, the chart depth datum, and the attitude correction.

In this paper, we propose a novel ocean bathymetry based on an USV, and test and validate it in sea experiments. The organization of this paper is as follows: the USBV is introduced in Section 2. The bathymetry technology based on USBV is described in Section 3. Section 4 describes an experiment, and the results and analyses are presented in Section 5. Finally, conclusions are provided in Section 6.

2 Unmanned surface bathymetry vehicle

The USBV was developed in the form of an inflatable catamaran with two propellers in the stern, with a length of 2.8 m, a width of 1.5 m, and weighing approximately 130 kg. The USBV design diagram is shown in Fig. 1. The maximum velocity of the USBV is 3 kn, and the endurance is approximately 20 km within a range of 5 h. The central control system and the lithium batteries are sealed separately in two stainless steel boxes, and the latter is fixed to the stern of the catamaran. On the basis of an embedded microcomputer, a central control system integrates a network RTK, a Trimble DSM232 DGPS, a Honeywell 3000 digital compass, a MicroStrain 3DM-GX3-25 IMU module, a single beam echo sounder, a camera, and a weather station. Two lithium batteries with capacities of 24 V 115 A·h and 12 V 20 A·h are used, respectively, as a power source for two thrusters and circuitry energy for the central control system with the above sensors. Two 24 V 400 W propellers are used as a propulsion system in the stern, which are controlled separately by two brushless DC actuators. The USBV steering is accomplished by regulating the revolving speed of two thrusters.

A shore-based control unit consists of wireless modules, a battery, a laptop, and control software. It is used to display callback data of depth, position, attitude, control state, and video from the USBV, and to send control commands. Further details of the USBV hardware are described in Jin et al. (2015).

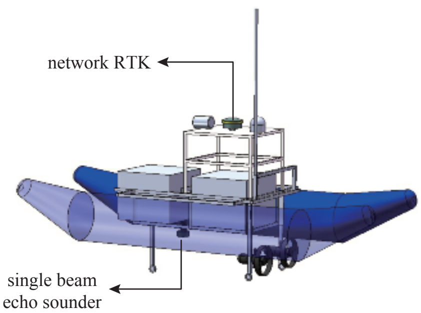

Fig. 1. The design diagram of the USBV integrating network RTK and a single beam echo sounder.

The network RTK (continuously operating reference stations) provides three-dimensional satellite navigation data with centimeter precision via the mobile network from public base stations in China, which are used to measure the instantaneous position and height of the USBV. The rover GPS antenna is mounted at 0.70 m above the plan of the waterline of the USBV (instantaneous sea level), and the single beam echo sounder is mounted at 0.10 m under the plan of the waterline of the USBV. The DGPS is used for the navigation of the USBV. The single beam echo sounder is an acoustic device for depth measurement with 1 cm accuracy within a range of 100 m. The Honeywell 3000 digital compass and the MicroStrain 3DM-GX3-25 IMU module can synthetically provide the heading, pitch, and roll output of the USBV with 0.5° accuracy.

The USBV control modes contain remote control, and an automatic following control for a course, way-point, and line, which can be tuned for different applications using the shore-based control unit. For example, the USBV is controlled automatically to converge onto an expected line using the control mode of automatically following a line. The automatic following control for a line is mainly used in the USBV depth measurement, which can form a “lawn mower” or line survey pattern.

3 Bathymetry technology for USV under tide and waves

The height of the USV with high precision in the long period can be used to obtain tidal and wave information, and the application is similar to a mobile GPS buoy. The chart depth can be acquired by removing tide and waves based on the instantaneous depth of the USV. However, the key problem to solve is how to obtain the distance between the reference ellipsoid datum and the chart datum, where the reference ellipsoid datum is the base level for the height of the RTK and the chart datum is the base level for the chart depth. Because of the effect of the curvature of the reference ellipsoid and the fluctuation of tide, the datum distance between the height and the depth varies in different regions. Furthermore, the survey missions allocated to the USV are usually short-term or emergent at present, and therefore the tidal information cannot be acquired from the measurement itself. Therefore, we propose a novel processing technology for the USV ocean bathymetry using available tidal information.

The relationship between the chart depth datum and the reference ellipsoid datum for the USV bathymetry is shown in Fig. 2, where D_g is the antenna height of the RTK calculated from the reference ellipsoid datum, D_u is the instantaneous depth of the USBV measurement, D_c is the chart depth calculated from the chart datum, $\triangle h_g$ is the height between the RTK antenna and the waterline of the USBV, $\triangle h_1$ is the distance between the chart depth datum and the reference ellipsoid datum, and $\triangle h_2$ is the distance between the instantaneous sea level and the chart depth datum.

In the USBV bathymetry system, the measurable data contain longitude, latitude, antenna height D_g from the network RTK, and instantaneous depth D_u from the echo sounder. Therefore, the variable to be solved is the chart depth D_c. According to the relationship from Fig. 2, the chart depth can be calculated by

$$D_c = D_u - \Delta h_2, \tag{1}$$

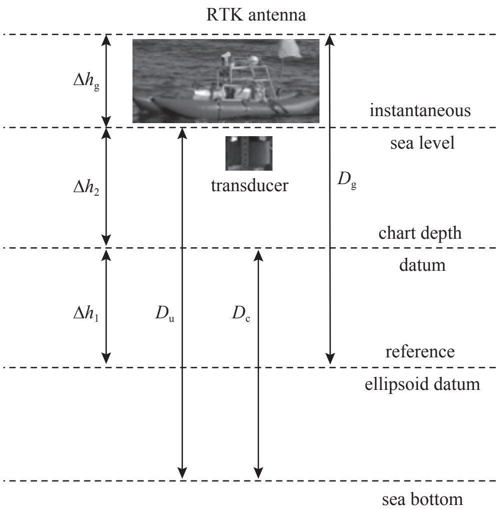

Fig. 2. Relationship in USBV bathymetry.

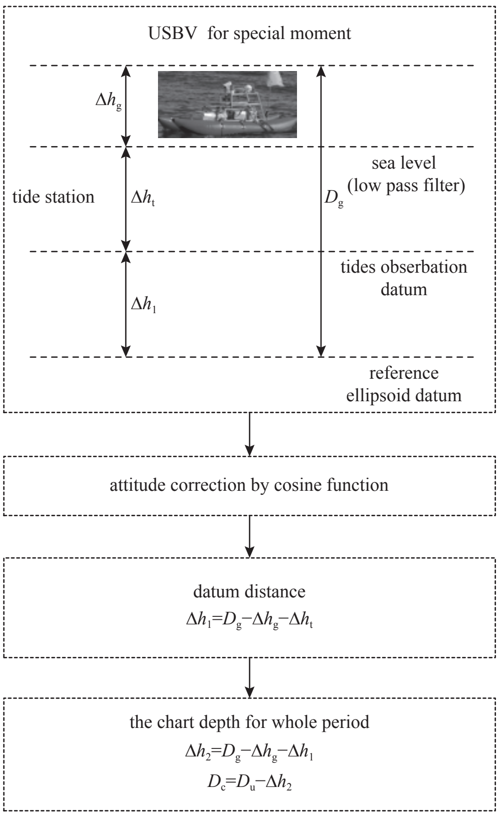

Fig. 3. A flowchart of the proposed technology.

$$\Delta h_2 = D_g - \Delta h_g - \Delta h_1. \tag{2}$$

Equations (1) and (2) are commonly used in the depth measurement by survey vessels, but problems occur when they are applied directly in the USV bathymetry. For example, the distance $\triangle h_1$ between the datum of the chart depth and the reference ellipsoid is difficult to measure directly by the USV. In traditional depth measurement missions, the datum distance is generally obtained from tide observations using a tide gauge, and the long period will be calculated, for example, over 1 month or longer. The traditional method for the tidal observations also limits the promotion and application of the USV. Survey missions allocated to the USV are usually short-term or emergent, and therefore the tidal information cannot be obtained from the traditional long-term tidal observations. Furthermore, the USV hours of operation are usually several hours in the daytime, and therefore few successive observations of tides are obtained. As a result, the calculation of the distance between the datum of the chart depth and the reference ellipsoid without the tidal observations is crucial to obtaining the chart depth for the bathymetry technology of the USV.

We propose a novel method to calculate the datum distance $\triangle h_1$ for the bathymetry technology of the USV. It is clear that the instantaneous sea level calculated from the chart datum contains the height of tide and waves (Fig. 2). The tide is a long-term process on the time-scale of hours, while a wave is a short-term process on the scale of seconds. Therefore, the height of tides can be obtained using a low pass filter of the instantaneous sea level (Vries, 2007; Apel et al., 2012). Tidal stations are generally fixed on the shore of a country, and can supply the height of tide $\triangle h_t$ calculated from the datum of the chart depth at a specific moment. The datum for tides coincides with the datum for the chart depth in China's tidal observations. Therefore, if a tide station is situated near the location of the USV mission and the height of the tide can be provided from tide stations in the period of the depth measurement, the distance $\triangle h_1$ between the datum of the chart depth and the reference ellipsoid equals the value of the height of the tide from the tide station subtracted from the height of the instantaneous sea level in the same moment, i.e.,

$$\Delta h_1 = D_g - \Delta h_g - \Delta h_t. \tag{3}$$

Within a specific range of region and period, the two datum distances $\triangle h_1$ can be considered a constant. Therefore, the chart depth can be calculated using Eqs (1) and (2). A flowchart of the proposed technology is illustrated in Fig. 3. All the heights will be corrected by the attitude data, which are provided by a three - dimensional digital compass.

4 Experiments

Application experiments for the USBV depth measurements were performed around Wuzhizhou Island on 3–6 January, 2016 (Fig. 4). Wuzhizhou Island is located at 18° 18′40″N, 109° 45′45″E, off the Haitang Bay, Sanya City, Hainan Province, which is 2.7 km offshore from the Haitang Bay (Fig. 5). Wuzhizhou Island is shaped like a butterfly, with an area of approximately 1.5 km^2.

During 4 d of experiments, the USBV was used for a total time and distance of approximately 16 h and 55 km, respectively. The USBV trajectories with instantaneous depth (denoted by a

Fig. 4. USBV in a sea trial.

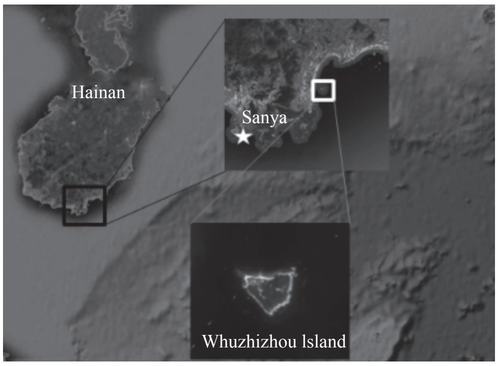

Fig. 5. Location of the experiments at the Wuzhizhou Island, Sanya City, China.

colored line) are shown in Fig. 6, where the largest successive time and distance for measurement were approximately 6 h and 20 km on the final day, respectively. In Fig. 6, the trajectories produced “lawn mower” curves and lines around Wuzhizhou Island. All the trajectories were achieved using automatic following of a line below the third level of the sea stage. The depth measurements show good agreement in continuity for successive trajectories and in the self-check for intersection points in a specific period. In Fig. 6, the maximum depth for the USBV measurement was approximately 30 m, while the minimum depth was about 0.5 m, which is close to the limit of the USBV for shallow running. After rejecting the false depth points, 13 797 depth points remained. In these data, a total number of 6 286 depths matched the position of the USBV with fixed solutions of the RTK. The fixed solutions of the RTK are the points with high precision that are corrected by the network differential signal in real time and all the positioning errors are less than 0.1 m. Because the differential signal is transmitted by the mobile phone network, most of the differential signals to the east of the island were lost, especially in the “lawn mower” sections.

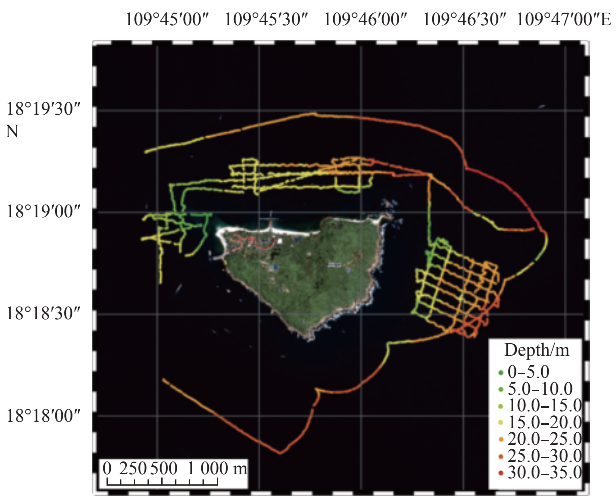

Fig. 6. USBV trajectories with instantaneous depth.

5 Results and analyses

5.1 *Effect of the USBV attitude error in depth measurement*

Because of waves and currents, the USBV attitudes that certain pitch and roll angles changed significantly in the experiments around Wuzhizhou Island compared with the attitude of the USBV in previous experiments in a lake (Jin et al., 2016). The pitch and roll angles of the USBV in the experiment on 3 January 2016 are shown in Fig. 7. The largest extent of the pitch and roll angles is about 10°, where the mean values of the pitch and roll angles are 2.4° and –3.0°, respectively, with corresponding standard deviations of 2.5° and 1.2°. The extent of the pitch for the USBV is about twice as large as the extent of the roll in the two figures. However, it is not common for the pitch angle to be greater than the roll angle in the experiments, because the attitudes of the USBV are affected by several issues, such as winds, waves, and currents. The USV was recovered transitorily by the mother ship between 11:30 and 11:50 because of the marine traffic control of the Wuzhizhou Island.

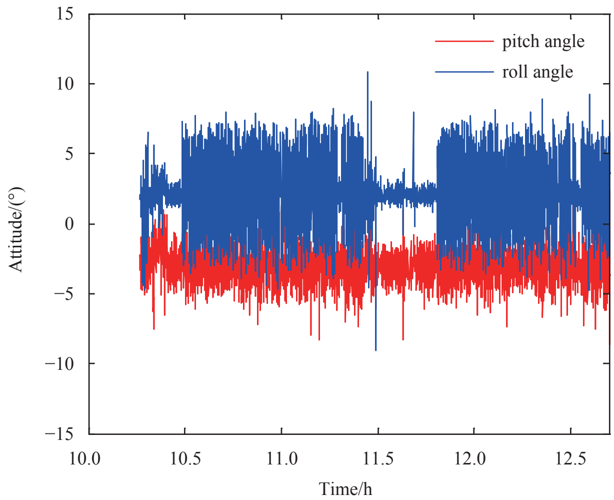

Fig. 7. Pitch and roll angles of the USBV.

Because of large fluctuations of the pitch and roll angles of the USBV, the depth had to be corrected using attitude angles. The attitude correction technology is discussed in full in previous surveys of ship depth measurement. We will therefore focus on the influence of the attitude error on the depth measurement of the USBV. Because of the attitude change of the USV in the ocean, the precision of the depth measurement is influenced by the error in the attitude measurement. On the basis of the cosine function of the USBV attitude and depth, the depth error of the echo sounder $\delta_{\rm d}$ caused by the error in the attitude measurement can be illustrated by

$$\delta_d = D\left(1 - \cos\left(\theta + \delta_\theta\right) / \cos\theta\right), \tag{4}$$

where D represents the depth of the echo sounder; θ and δ_θ represent the attitude angle and its measurement error, respectively.

According to Eq. (4), when the desired depth error $\delta_{\rm d}$ is 0.2%D and the attitude error of the USBV δ_θ is 0.5°, the attitude angle range for the USBV θ should be less than 12.7°. Therefore, if the precision of the compass is 0.5° and that of the echo sounder is 0.2%D, the depth measurement for the USBV is valid on the condition that the attitude extent of the USV is less than 12.7°, and vice versa. If the precision of the depth measurement is expected as 0.1%D and 0.2%D, respectively, the relationship between the allowable measurement error for the attitude and the maximum allowable attitude angle extent for the two cases are shown in Fig. 8.

When the attitude angle of the USBV increases, i.e., the level of the sea stage enhances, the allowable measurement error for the USBV attitude will decrease, i.e., the precision of the compass should improve. In Fig. 8, the largest extent of the USBV attitude is approximately 10°, with a standard deviation of 2.5°. In the USBV, the precision of the Honeywell 3000 digital compass is 0.5°. Therefore, if the maximum allowable extent of the attitude angle for the USBV is 6.3° and 12.7° for the two cases of 0.1%D and 0.2%D depth measurement error, respectively, then the depth measurement error of the USBV fully satisfies 0.2%D and basically satisfies 0.1%D, because the largest extent of the attitude angle of the USBV is approximately 10° (Fig. 7).

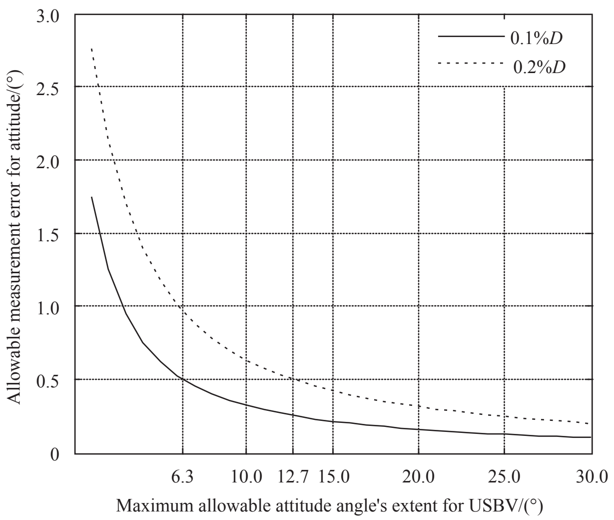

Fig. 8. Relationship between the allowable measurement error for the attitude and the maximum allowable extent of the attitude angle for the USBV.

5.2 *Acquisition of chart depth for the USBV*

In these experiments, 6 286 depth points matched the position of the USBV with fixed solutions of the RTK, and all the RMSs of the fixed solutions of the RTK were less than 0.1 m. The histogram for the RMS of the fixed solutions of the RTK is shown in Fig. 9. In this figure, the vast majority of the RMS values of the fixed solutions were less than 5 cm, and the mean of RMSs of the fixed solutions of the RTK was 2 cm. These data therefore have high precision, which indicates that the tide can be obtained accurately.

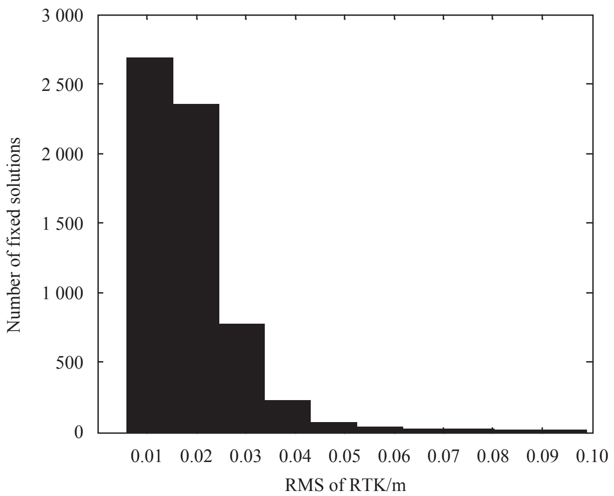

Fig. 9. Histogram of the RMS of the fixed solutions of the RTK.

Rejecting the length of the antenna of the RTK, the instantaneous height of the USBV consists of the wave and tidal heights. Because the tidal period is much longer than the wave period, the tidal height can be obtained using a low pass filter for the height of the USBV, which also represents the sea level. The heights of the USBV and the sea level from 3 to 6 January are shown in Fig. 10. The blue line represents the instantaneous height of the USBV, and the red line represents the height of the sea level using a low pass filter. A digital Chebyshev Type I filter was used as the low pass filter for the height of the USBV. Because the tidal periods last several hours and the wave periods only several minutes, we choose pass - band and stop - band frequencies of 0.000 1 and 0.001, respectively. The low pass filter confirms that the height of the sea level will be obtained correctly by removing the wave signal. All the heights were calculated from the datum of the reference ellipsoid in Fig. 10.

According to the tide table released by the National Ocean Information Center of China, the sea level calculated from the datum of the chart depth at the Yalong Harbor was 0.66 m at 10:36 on 3 January 2016, with the Yalong Harbor as the nearest tidal station to the Wuzhizhou Island (labeled with a white star in Fig. 5). At the same time, the sea level calculated from the datum of the reference ellipsoid was –9.70 m (Fig. 10a). This indicates that the sea level is between the datum of the reference ellipsoid and the datum of the chart depth. According to Eq. (3), the distance between the datum of the chart depth and the reference ellipsoid $\triangle h_1$ is –10.36 m. Some measurements in Fig. 10b were not successive because of the recovery of the USBV. Using the same method, the two datum distance $\triangle h_1$ can be calculated from 4 January to 6 January (Table 1). The $\triangle h_1$ values were similar on 3 and 4 January, but there was a 20–30 cm difference compared with the $\triangle h_1$ values on 5 and 6 January (Table 1). The $\triangle h_1$ values were calculated using the height of the sea level from the Yalong Harbor Tidal Station on 3 and 4 January at the same time. However, the heights of the sea level on 5 and 6 January were calculated using the interpolated results from the tide tables, because no measurement was available at the corresponding time. Therefore, the $\triangle h_1$ values on 3 and 4 January were taken as the valid ones, and the precision for the distance between the datum of the depth and the reference ellipsoid can be taken as approximately 4 cm. In the area where the experiments for the USBV were carried out, the two datum distance $\triangle h$ is considered to be constant.

Using Eqs (1) and (2), the chart depth for the USBV was calculated based on the $\triangle h_1$ value. The result is illustrated using the depth measurement for the USBV on 3 January as an example. The instantaneous and the chart depths are compared in Fig. 11, and the trajectory for the USBV with the chart depth is shown in Fig. 12. In the USBV measurement, the echo sounder and the RTK were synchronized according to the central control computer time. The echo sounder measurement frequency was set to 1 Hz during the experiments, and the RTK measurement frequency was set to 1 Hz on 3 and 4 January, and to 0.2 Hz on 5 and 6 January. The chart depth was calculated using the RTK measurement frequency to match the two devices. In Fig. 11, the chart depth is less than the instantaneous depth because of the removal of tide and waves from the instantaneous depth.

During 4 d of experiments, less than half of the RTK data were fixed solutions with high precision in Fig. 13, where the green line

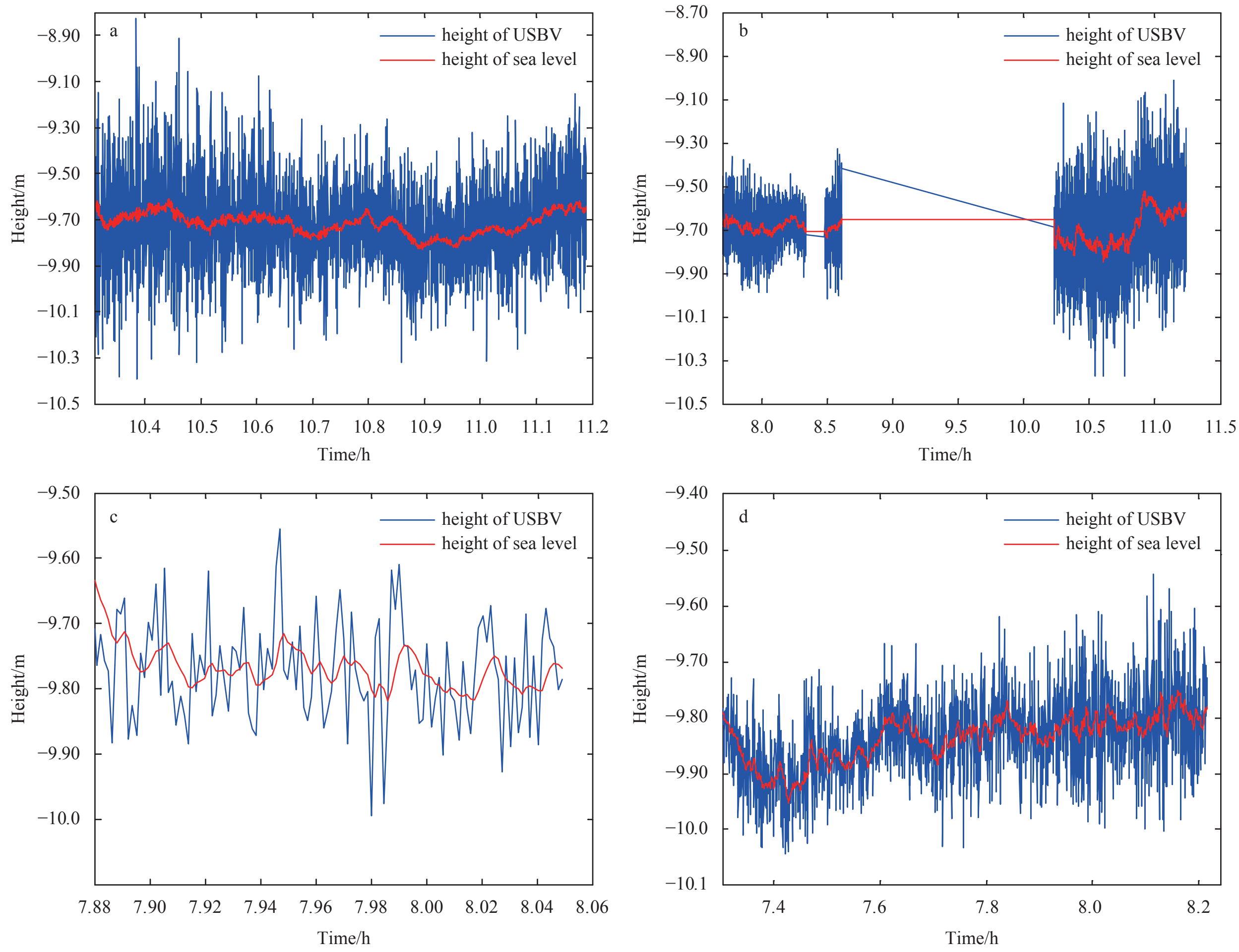

Fig. 10. Heights of sea level for 3–6 January 2016 (a–d) using the USBV.

Table 1. Distance between the datum of the chart depth and the datum of the reference ellipsoid

Date	Time	h_t/m	D_g–h_g/m	$\triangle h_1$/m
3 January 2016	10:36	0.66	–9.70	–10.36
4 January 2016	10:51	0.72	–9.68	–10.40
5 January 2016	08:00	0.81	–9.78	–10.59
6 January 2016	08:04	0.86	–9.79	–10.65

represents the position of the USBV with the fixed solutions of the RTK, and the red line represents the position of the USBV with the non-fixed solutions of the RTK due to the lack of a differential signal from the network. The result for the chart depth on 4 January is shown in Fig. 14. The results for 5 and 6 January are not included because of the lack of sufficient fixed solutions from the RTK. In Fig. 14, some of the USBV trajectories are also missing. Although the data over the first 2 d are enough to validate the proposed technology, it is unfortunate for the USBV bathymetry application. It is clear that the chart depth produced by the proposed technology has favorable continuity in Figs 11, 12 and 14.

Because the experiments with the USBV around the Wuzhizhou Island were made on a small-scale ocean map with high precision measurements in the super - nearshore, it is difficult to find available data produced by traditional methods using ship investigations in the same area. However, the cross lines for the USBV are designed and performed to achieve cross point inspection in the experiments. There are not many effective cross points in Fig. 13, because most of the design cross lines are located east of the island with non-fixed solutions of the RTK. However, some cross points can still be found and are illustrated in Table 2, and the mean value of the depth errors for the six cross points is approximately 0.05 m. The contribution of the depth error to the cross points is explained by two aspects; one is the precision of the GPS height for the RTK with 2–3 cm accuracy, and the other is the precision of the echo sounder with 1–2 cm accuracy.

6 Conclusions

A novel bathymetry technology based on an USV with little tide information is proposed for ocean bathymetry. Sea trials were used to validate the proposed technology for depth measurements using the USBV around the Wuzhizhou Island in Hainan Province, China. The free tide information released by the National Ocean Information Center of China and the height of the instantaneous sea level measured by the USBV were successfully used to obtain the constant distance between the datum of the chart depth and the reference ellipsoid. The chart depth for the USV is achieved using traditional bathymetry without tidal obser-

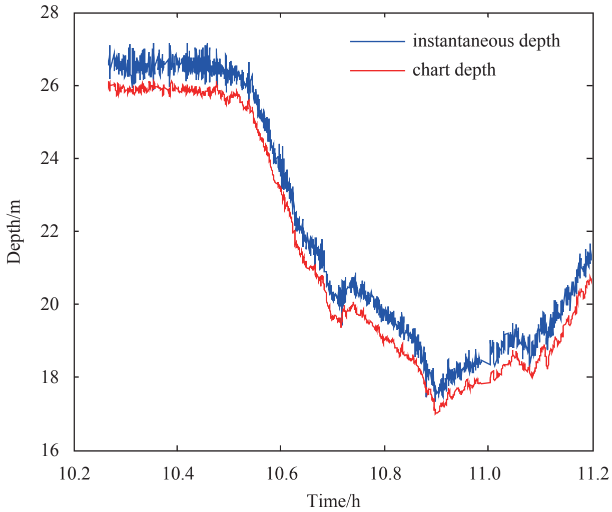

Fig. 11. Comparison of the instantaneous and chart depths.

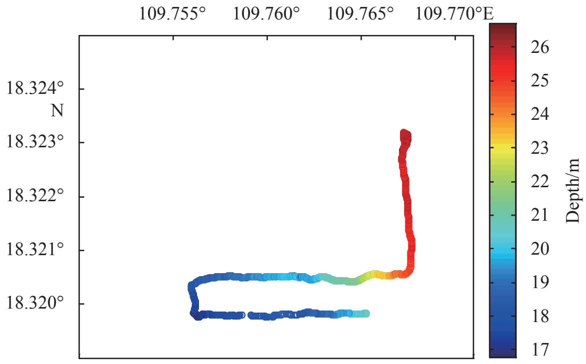

Fig. 12. Trajectory of the USBV with chart depth on 3 January.

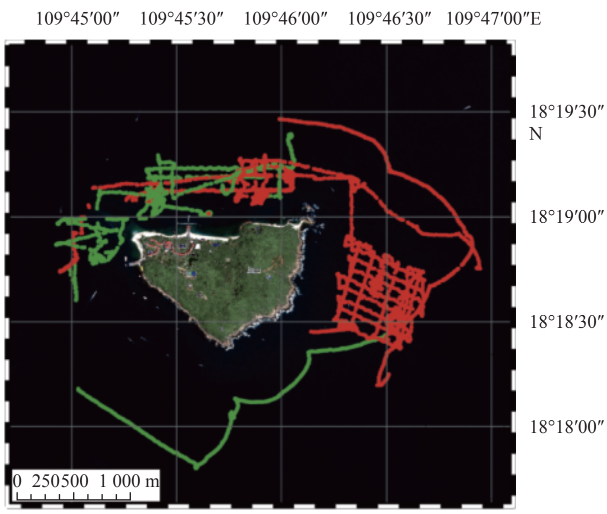

Fig. 13. The position of the USBV with fixed and non-fixed solutions of the RTK. The green line represents the position of the USBV with fixed solutions, and the red line with non-fixed solutions.

vations. The proposed technology is simple and feasible, and can provide a significant reference for the application of the USV depth measurements in the future.

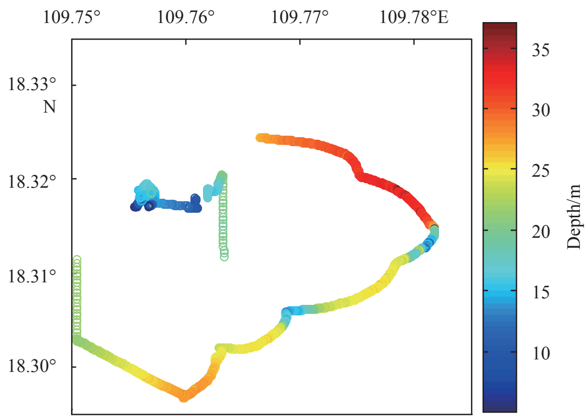

Fig. 14. Trajectory of the USBV with chart depth on 4 January.

Table 2. Inspection of cross points

No.	Cross points' location	Depth error/m
1	18°19′05″ N, 109°45′ 22″E	0.09
2	18°19′07″ N, 109°45′ 21″ E	0.04
3	18°19′08″ N, 109°45′ 26″ E	0.01
4	18°19′01″ N, 109°45′ 39″ E	0.08
5	18°18′45″ N, 109°44′ 58″ E	0.04
6	18°18′38″ N, 109°45′ 01″ E	0.03

Acknowledgements

The authors thank Ma Yi and Liang Jian from The First Institute of Oceanography, State Oceanic Administration of China for CORS GPS technology support and assistance with experiments.

References

Annamalai A S K, Sutton R, Yang Chengguang, et al. 2015. Robust adaptive control of an uninhabited surface vehicle. Journal of Intelligent & Robotic Systems, 78(2): 319–338
Apel H, Hung N G, Thoss H, et al. 2012. GPS buoys for stage monitoring of large rivers. Journal of Hydrology, 412: 182–192
Bibuli M, Bruzzone G, Caccia M, et al. 2014. Unmanned surface vehicles for automatic bathymetry mapping and shores' maintenance. In: Proceedings of 2014 MTS/IEEE Oceans Conference. Piscataway, New Jersey: IEEE Press, 1–7
Brown H C, Jenkins L K, Meadows G A, et al. 2010. BathyBoat: an autonomous surface vessel for stand-alone survey and underwater vehicle network supervision. Marine Technology Society Journal, 44(4): 20–29
Bruzzone G, Bibuli M, Caccia M. 2011. Improving coastal operations with unmanned surface vehicles. Sea Technology, 52(7): 46–49
Hostache R, Matgen P, Giustarini L, et al. 2015. A drifting GPS buoy for retrieving effective riverbed bathymetry. Journal of Hydrology, 520: 397–406
Jin Jiucai, Zhang Jie, Ma Yi, et al. 2013. Analysis for unmanned surface bathymetric vehicle's spatial-temporal sampling character and equal distance parallel formation control. International Journal of Advanced Robotic Systems, 10(7): 285: 1–6
Jin Jiucai, Zhang Jie, Shao Feng. 2015. Modelling, manoeuvring analysis and course following for two unmanned surface vehicles driven by a single propeller and double propellers. In: Proceedings of 27th Chinese Control and Decision Conference. Piscataway, New Jersey: IEEE Press, 4952–4957
Jin Jiucai, Zhang Jie, Shao Feng, et al. 2016. Active and passive underwater acoustic applications using an unmanned surface vehicle. In: Proceedings of 2016 MTS/IEEE Oceans Conference. Piscataway, New Jersey: IEEE Press, 1–6
Kebkal K G, Kebkal O G, Glushko I, et al. 2014. SONOBOT —an autonomous unmanned surface vehicle for hydrographic sur-

veys, hydroacoustic communication and positioning in tasks of underwater acoustic surveillance and monitoring. In: Proceedings of 2nd International Conference and Exhibition on Underwater Acoustics. Tokyo: Marine Acoustics Society of Japan, 221–222

Liu Zhixiang, Zhang Youmin, Yu Xiang, et al. 2016. Unmanned surface vehicles: an overview of developments and challenges. Annual Reviews in Control, 41: 71–93

Lü Zhichao, Zhang Jie, Jin Jiucai, et al. 2016. Link strength for unmanned surface vehicle's underwater acoustic communication. In: Proceeding of 2016 IEEE/OES China Ocean Acoustics Symposium. Piscataway, New Jersey: IEEE Press, 1–4

Manley J E, Marsh A, Cornforth W, et al. 2000. Evolution of the autonomous surface craft AutoCat. In: Proceedings of 2000 MTS/IEEE OCEANS Conference. Providence. IEEE Press, 403–408

Rodriguez-Ortiz C D. 1996. Automated bathymetry mapping using an autonomous surface craft [dissertation]. Massachusetts: Massachusetts Institute of Technology

Seto M L, Crawford A. 2015. Autonomous shallow water bathymetric measurements for environmental assessment and safe navigation using USVs. In: Proceedings of 2015 MTS/IEEE Oceans Conference. Piscataway, New Jersey: IEEE Press, 1–5

Shojaei K. 2015. Neural adaptive robust control of underactuated marine surface vehicles with input saturation. Applied Ocean Research, 53: 267–278

Vries J J D. 2007. Designing a GPS-based mini wave buoy. International Ocean Systems, 11(3): 20–23

Zhu Jing, Wang Jianhua, Zheng Tiqiang, et al. 2016. Straight path following of unmanned surface vehicle under flow disturbance. In: Proceedings of 2016 MTS/IEEE Oceans Conference. Piscataway, New Jersey: IEEE Press, 1–7